

Supporting Information

Lagace et al. 10.1073/pnas.0910072107

SI Methods

Animals. Adult (5–8 weeks of age) male mice expressing GFP under the control of the nestin promoter (2) were used in this study. For the social defeat paradigm, the aggressor mice were CD1 retired breeders (Charles River). In three consecutive screening trials before the start of the defeat paradigm, aggressors were selected based on a requirement to attack a C57BL/6 mouse in less than 30 sec. Mice were housed in a facility approved by the American Association for the Accreditation of Laboratory Animal Care International at the University of Texas Southwestern Medical Center with a 12-hr light/dark cycle and ad libitum access to food and water.

Social Defeat and Social Interaction Protocol. The social defeat and interaction testing was performed as described previously (3–5). A CD1 aggressor mouse was housed on one side of a cage that was partitioned with a plastic divider throughout the 10 days of defeat stress. A test mouse was housed on the other side of the divider. The defeat was performed 2–3 hr before the onset of the dark phase of the light cycle. During the 5-min defeat period, the test mouse was moved to the side of the cage housing the aggressor, which would physically attack the test mouse. Test mice were rotated so that after each defeat period, test mice were housed in a different cage living opposite a different aggressor. Control mice were housed in partitioned cages identical to those used for defeat; however, instead of being housed beside an aggressor, they were housed opposite to other control mice. Control mice were handled each day at the same time of day as when the defeat was performed throughout the 10 days.

Social interaction was measured in the morning between 0800 and 1200 hours and consisted of two trials lasting 150 sec each. Using Ethovision software (Noldus Information Technology), the movements of the test mouse were tracked within a white open-field box (45 cm long × 45 cm wide × 30 cm high). Within the box, an interaction zone (26 cm wide × 14 cm long) was defined, and a plastic enclosure (10 cm × 6 cm) was placed in the center of the interaction zone against the wall of the box. In each trial, the mouse was placed randomly into either one of the corners of the box on the side opposite to the interaction zone. In the first trial, the test mouse was placed into the open area with the empty enclosure in the interaction zone. The time that the mouse spent either in the interaction zone or in corners opposite from the interaction zone was quantified. In the second trial, the same measurements were taken; however, unlike the first trial, an unfamiliar CD1 aggressor mouse was placed into the enclosure. The interaction ratio was calculated as follows: (time spent in interaction zone with aggressor mouse/time spent in interaction zone with empty enclosure present) × 100. Immediately after testing for social interaction, all mice were singly housed until they were euthanized.

Passive Avoidance Task. The passive avoidance task determines the ability of a mouse to remember a foot shock delivered 24 hr earlier. Our protocol was similar to that followed in other published work (6). This test was completed using the shuttle box apparatus and software from Med Associates. Mice were habituated to the behavioral testing area for 1 hr before training and testing. For training, a mouse was placed in the chamber with the lights on. After 2 min, the automatic guillotine door opened to allow the mouse access to the dark chamber. Once the mouse entered the dark chamber, the guillotine door closed and a single foot shock was delivered through the grid floor (0.5 mA, 2 sec). The mouse was kept in the dark chamber for an additional 1 min before being

returned to its home cage to allow the animal to form an association between the properties of the chamber and the foot shock. During testing, which was performed 1 day after training, the mouse was placed back into the same light compartment with the guillotine door already open. The time taken (the step-through latency) for the mouse to enter the dark compartment was recorded. The maximum test latency was set at 700 sec; at that time, the test was discontinued.

Juvenile Interaction. The juvenile social interaction test measures the interaction between an adult test mouse and a juvenile mouse (4–5 weeks of age and of the same gender and strain as the adult mouse). Similar to previously published methods (7), we determined the social interaction in an empty, clear, plastic mouse cage under red light conditions. Following a 15 min habituation period in the home cages to the testing room and red light condition, the experimental and juvenile mice were placed in the neutral cage at the same time in opposite ends of the cage and allowed to interact freely for 2 min. The time the adult spent interacting with the juvenile (approaching, following, sniffing, climbing onto, and grooming) was scored by an observer blinded to genotype. Social learning was assessed 3 days later by repeating the same protocol and allowing mice to interact with the same juvenile for an additional 2 min. Again, time spent interacting with the juvenile was scored.

Ablation of Neurogenesis Using X-Ray Irradiation. Ionizing radiation was carried out using the X-RAD 320 self-contained irradiation system (Precision X-Ray, Inc.). The X-RAD 320 irradiator is equipped with a custom-synthesized collimator that delivered an x-ray beam of 10 mm in diameter at rate of 1.08 Gy/min (250 kV, 15 mA) for 4.5 min to achieve the cumulative desired dose of 5 Gy. Mice were anesthetized with ketamine/xylazine (9 mg/kg and 1 mg/kg in saline, respectively) before being positioned in an irradiator with their skulls located under collimator for whole-head irradiation. For sham-irradiated controls, anesthetized mice were positioned in the irradiator but the device was never turned on. Following irradiation, mice recovered on a heating pad and were returned to previous housing conditions when fully awake.

CORT Measurements. Blood samples were centrifuged (1,000 × g for 15 min), and plasma was frozen at –20 °C until assayed for CORT levels using the mouse OCTEIA CORT competitive enzyme immunoassay (Immunodiagnostic System) (8).

BrdU Injection, Tissue Collection, and Processing. Mice received an i.p. injection of BrdU (150 mg/kg; Boehringer Mannheim) before being euthanized to label proliferating cells in the S-phase of the cell cycle. The time between BrdU injection and death varied across experimental groups (+1 min-P, +24 hr-P, –12 hr-S, +24 hr-S; Fig. 3A, Fig. 4A, and *SI Text*). For proliferation analyses, this time was under the estimated length of G2 (4–5 hr) (9, 10); thus, it is not surprising that there was no difference in BrdU-IR cell number between 30 min and 2 hr (11). BrdU injection occurred in each group 10 hr following social interaction testing, except for +1 min-P, when mice were injected immediately after defeat and euthanized 30 min later. For the +24 hr-P and +24 hr-S, BrdU was given 24 hr following the last defeat and mice were euthanized either 2 hr or 4 weeks following BrdU injection, respectively.

Tissue Collection. All mice were euthanized between 1600 and 1900 hours. Mice were decapitated, blood was collected for CORT analysis, and brains were cut along the midsagittal sulcus. One hemisphere was immersion-fixed for immunohistochemistry (IHC;

Fig. S9), and the other was used for hippocampal dissection and subsequent protein content analyses via Western blot (Fig. S7). For immersion fixation, hemispheres were placed in 4% paraformaldehyde (PFA; wt/vol) in 0.1 M PBS for 3 days with PFA changed daily. Immersion-fixed tissue was viable for all IHC applications, and there were no differences between immersion-fixed and perfused tissue in any measures of IR cells (Fig. S9).

IHC. After immersion fixing in PFA, brains were subsequently cryoprotected in 30% sucrose (wt/vol) in 0.1 M PBS and 0.1% sodium azide (NaN_3 ; wt/vol) and sectioned coronally on a freezing microtome (Leica) at 30 μm through the hippocampus. Nine serial sets of sections were stored in 0.1% NaN_3 in 1 \times PBS at 4 °C until processing. For staining, one series of sections was ordered from rostral to caudal, mounted on glass slides (Superfrost/Plus; Fisher), and dried overnight. Slides were coded to ensure objectivity, and the code was not broken until after data collection was complete.

For BrdU IHC, pretreatment consisted of antigen retrieval (0.01 M citric acid, pH 6.0, 95 °C, 10 min), membrane permeabilization (0.1% trypsin in 0.1 M Tris and 0.1% CaCl_2 , 10 min), and DNA denaturation (2 N of hydrochloric acid in 1 \times PBS, 30 min). For the DCX IHC, pretreatment consisted of only antigen retrieval. Following pretreatment, nonspecific staining was blocked by incubation with 3% normal donkey serum (NDS; vol/vol) in 0.1% Triton X-100 in 1 \times PBS. Sections were incubated in either rat anti-BrdU primary antibody (1:300; Accurate Chemical) or goat anti-DCX (1:1,000; Santa Cruz) in 3% NDS (vol/vol) in 0.1% Tween-20 in 1 \times PBS overnight. The following day, sections were incubated with biotinylated-donkey anti-rat or biotinylated-donkey anti-goat secondary antibody (1:200; Sigma Laboratories) in 1.5% NDS (vol/vol) for 60 min, 0.3% hydrogen peroxide (Sigma Laboratories) for 30 min, and avidin-biotin complex (ABC; Vector Laboratories) for 90 min. Staining of BrdU and DCX IR cells was visualized using DAB (Pierce) for 20–30 min. Nuclear Fast Red (Vector Laboratories) was used as a counterstain.

AC3 IHC pretreatment was the same as BrdU pretreatment as described previously. Following pretreatment, nonspecific staining was blocked by incubation with 3% NDS (vol/vol) in 0.1% Triton X-100 in 1 \times PBS. Sections were incubated in rabbit polyclonal anti-AC3/cleaved caspase-3 (1:500; Cell Signal) 3% NDS (vol/vol) in 0.1% Tween-20 in 1 \times PBS overnight. The following day, sections were incubated with donkey anti-rabbit fluorophore-conjugated secondary antibody (1:200, CY3; Jackson ImmunoResearch) for 3 hr and counterstained with DAPI (1:5,000; Roche).

For BrdU/NeuN/GFAP triple-labeling immunofluorescent staining, sections were pretreated as described previously and nonspecific labeling was blocked with 3% NDS for 60 min before overnight incubation with rat anti-BrdU, mouse anti-neuronal nuclei (NeuN, 1:50; Chemicon International), and rabbit anti-GFAP (1:500; DAKO). Sections were then incubated in fluorescent CY2-donkey anti-rat, CY5-donkey anti-rabbit, and CY3-goat anti-mouse secondary antibodies (1:200; Jackson ImmunoResearch) for 3 hr and counterstained with DAPI (1:5,000).

For BrdU/Ki67 double-labeling fluorescent IHC, sections underwent antigen retrieval (first step of pretreatment), followed by blocking of nonspecific staining in 3% NDS (vol/vol) for 60 min before overnight incubation with rabbit anti-Ki67 (1:1,000, Vector Laboratories). Sections were then incubated in biotinylated-donkey anti-rabbit (1:200; Vector Laboratories) and amplified by ABC and CY3-tyramide signal amplification (TSA; Perkin-Elmer), followed by membrane permeabilization and DNA denaturation (the second and third pretreatment steps), blocking again in 3% NDS (vol/vol) for 60 min, and a second overnight incubation with rat anti-BrdU, detected as above, with fluorescent CY2-donkey anti-rat.

Similarly, for BrdU/GFP/DCX triple-labeling fluorescent IHC, sections underwent antigen retrieval, blocking of nonspecific staining in 3% NDS (vol/vol) for 60 min, and overnight incubation with rabbit anti-GFP (1:3,000; Abcam) and goat anti-DCX (1:5,000).

This was followed by sequential incubation in 0.3% hydrogen peroxide, biotinylated-horse anti-goat (1:200; Vector Laboratories), ABC, and CY5-TSA, followed by 0.3% hydrogen peroxide again, biotinylated-donkey anti-rabbit (1:200), ABC, and CY3-TSA. Finally, the sections were incubated again in 3% NDS (vol/vol) for 60 min and a second overnight incubation with primary rat anti-BrdU antibody, and signal was detected on day 3 with fluorescent CY2-donkey-anti-rat antibody.

Stereological Cell Counting. Bright-field or epifluorescent staining of sections on coded slides was visualized and quantified with an Olympus BX-51 microscope. Staining was examined and quantified in several regions of the dentate gyrus of the hippocampus (bregma: -0.82 to -4.24), including the SGZ, molecular layer (Mol), polymorphic layer (hilus), and outer granular cell layer (oGCL) (1, 12). The SGZ has been shown to give rise to cells with neurogenic potential, and therefore was the focus of these studies for BrdU-, Ki67-, DCX-, and AC3-IR as well as for Type-1 cell counts. The other hippocampal regions were assessed to control for bioavailability of the exogenous marker BrdU (13) to augment our previous work on the proliferative capacity and regulation of proliferation of these neighboring dentate gyrus regions (14), and thus to explore the regional specificity of stress-induced effects. The SGZ was defined as a region straddling the border of the granular cell layer (GCL) and the hilus: three GCL cell widths into the hilus and the inner half of the GCL adjacent to the hilus. The Mol was defined as the region between the superior limb of the GCL and the hippocampal fissure and the inferior limb of the GCL and the ventral and medial borders of the DG; inner and outer Mol results were combined for this study. A cell on the border in the middle of the GCL was considered to be in the SGZ, whereas a cell touching the GCL on the border of the Mol was considered to be in the oGCL. A schematic of the anterior hippocampus (-2.18 from bregma) depicting the four dentate gyrus regions analyzed is shown in Fig. S2. However, the hippocampus across the septotemporal axis (-0.82 to -4.24 from bregma) was analyzed for this study.

The quantification of IR cells in the SGZ, Mol, oGCL, and hilus was performed using stereology (15, 16) by an examiner blinded to treatment. Using an Olympus BX-51 microscope at $\times 400$ magnification and continual adjustment through the depth of the section, IR cells in each dentate gyrus subregion were counted in every ninth section through the septotemporal axis of the hippocampus. The section sampling fraction was 1/9, and the resulting number for each region was multiplied by 9 to obtain an estimate of the total number of cells per dentate gyrus subregion. Because the raw counts (before multiplication) for the IR cells counted here were low according to disector/fractionator standards (17–19), we used an area sampling fraction of 1 as is commonly used for counting rare populations of cells (16, 20). Based on the previous work from our laboratory and those of others (15, 20–23), the height sampling fraction was set at 1. As previously described by our laboratory and those of others (11, 24), BrdU- and Ki67-IR cells within clusters were resolved by distinguishing nuclear (BrdU, Ki67) borders with an objective with appropriate working distance. AC3-IR cells were resolved as previously described [in particular, in the article by Harburg et al. (25)]. For Type-1 cell analysis, GFP-IR cells with a radial process perpendicular to the SGZ were similarly quantified by a single observer blinded to experimental condition. In addition to estimating the total number of IR cells across the entire hippocampus, the distribution of cells across the longitudinal axis of the hippocampus was analyzed as different distances from the bregma, and data are presented as total number of cells in the SGZ per section at each septotemporal point (12).

IR-Cell Phenotyping. Colocalization of immunofluorescence was determined with a confocal microscope (Axiovert 200 and LSM510-META; Carl Zeiss; emission wavelengths of 488, 543, and 633 nm) at $\times 630$ magnification using multitrack scanning and an optical

section thickness of $\approx 0.5 \mu\text{m}$ in the z plane. To guard against false-positive results (26), colocalization was verified by importing Z-stacks of images into a 3D reconstruction program (Volocity; Improvision). The 3D renderings were rotated and examined from multiple perspectives to ensure colocalization. For presentation, images were imported into Photoshop (Adobe Systems) and adjustments were made only via the “level” function. To assess the putative stages of neurogenesis, we examined the colocalization of BrdU-IR cells with DCX and GFP and analyzed the DCX and GFP morphology to identify four distinct cell types that represent putative stages and potential lineages of hippocampal neurogenesis (e.g., 9, 27, 28). We identified stem-like cells (Type-1) as GFP-IR/DCX with radial glial-like morphology; early progenitors (Type-2a) as GFP-IR/DCX with compact morphology; late progenitors (Type-2b) as GFP-IR/DCX-IR with compact morphology; and progenitors/neuroblasts (Type-3) as GFP/DCX-IR. Fig. S8 provides examples of these cell types.

Protein Extracts and Western Blot Analysis. The hippocampus from the remaining hemisphere of each mouse was rapidly dissected and frozen at -80°C until processed. Extracts were homogenized by sonication and boiled in 1% SDS with 50 mM sodium fluoride.

- Mandyam CD, Norris RD, Eisch AJ (2004) Chronic morphine induces premature mitosis of proliferating cells in the adult mouse subgranular zone. *J Neurosci Res* 76:783–794.
- Yamaguchi M, Saito H, Suzuki M, Mori K (2000) Visualization of neurogenesis in the central nervous system using nestin promoter-GFP transgenic mice. *NeuroReport* 11: 1991–1996.
- Berton O, et al. (2006) Essential role of BDNF in the mesolimbic dopamine pathway in social defeat stress. *Science* 311:864–868.
- Tsankova NM, et al. (2006) Sustained hippocampal chromatin regulation in a mouse model of depression and antidepressant action. *Nat Neurosci* 9:519–525.
- Krishnan V, et al. (2007) Molecular adaptations underlying susceptibility and resistance to social defeat in brain reward regions. *Cell* 131:391–404.
- Kim JS, et al. (2008) Transient impairment of hippocampus-dependent learning and memory in relatively low-dose of acute radiation syndrome is associated with inhibition of hippocampal neurogenesis. *J Radiat Res* 49:517–526.
- Tabuchi K, et al. (2007) A neuroligin-3 mutation implicated in autism increases inhibitory synaptic transmission in mice. *Science* 318:71–76.
- Lagace DC, Yee JK, Bolaños CA, Eisch AJ (2006) Juvenile administration of methylphenidate attenuates adult hippocampal neurogenesis. *Biol Psychiatry* 60: 1121–1130.
- Cameron HA, McKay RD (2001) Adult neurogenesis produces a large pool of new granule cells in the dentate gyrus. *J Comp Neurol* 435:406–417.
- Hayes NL, Nowakowski RS (2002) Dynamics of cell proliferation in the adult dentate gyrus of two inbred strains of mice. *Brain Res Dev Brain Res* 134:77–85.
- Mandyam CD, Harburg GC, Eisch AJ (2007) Determination of key aspects of precursor cell proliferation, cell cycle length and kinetics in the adult mouse subgranular zone. *Neuroscience* 146:108–122.
- Franklin K, Paxinos G (2001) *The Mouse Brain in Stereotaxic Coordinates* (Elsevier, San Diego), 3rd Ed.
- Noonan MA, Choi KH, Self DW, Eisch AJ (2008) Withdrawal from cocaine self-administration normalizes deficits in proliferation and enhances maturity of adult-generated hippocampal neurons. *J Neurosci* 28:2516–2526.
- Eisch AJ, Mandyam CD (2007) Adult neurogenesis: Can analysis of cell cycle proteins move us “Beyond BrdU”? *Curr Pharm Biotechnol* 8:147–165.

Protein concentrations were determined by bicinchoninic acid assay (Pierce). Forty micrograms of total protein from each sample was electrophoresed on precast 4–20% SDS gradient gels (BioRad). Following transfer, PVDF membranes were washed for 1 hr in 1× Tris-buffered saline with 0.1% Tween-20 and blocked in 5% (wt/vol) milk for 1 hr at 25°C . The membrane was then incubated in a solution of the appropriate primary antibody overnight at 4°C . Antibodies used included anti-BDNF (N-20, 1:200; Santa Cruz), anti-TrkB (07-225, 1:4,000; Upstate), anti-ERK 1/2 (4695, 1:1,000; Cell Signaling), and anti-ERK1/2 (4377, 1:1,000; Cell Signaling). On the second day, blots were washed and then incubated with peroxidase-labeled secondary antibody at 25°C for 1 hr and bands were visualized by enhanced chemiluminescence (Amersham, GE Healthcare). Results were quantified using National Institutes of Health image software.

Statistical Analyses. Data are reported as mean \pm SEM for control, susceptible, and unsusceptible groups. Experiments with two groups were analyzed using an unpaired *t* test. Three or more groups were analyzed with a multiple variable ANOVA, followed by a Bonferroni post hoc test. All statistical analyses were performed using either SPSS (version 11.0.2) or Prism software, and statistical significance was defined as $P < 0.05$.

- Eisch AJ, Barrot M, Schad CA, Self DW, Nestler EJ (2000) Opiates inhibit neurogenesis in the adult rat hippocampus. *Proc Natl Acad Sci USA* 97:7579–7584.
- Mouton P (2002) *Principles and Practices of Unbiased Stereology: An Introduction for Bioscientists* (Johns Hopkins Univ Press, Baltimore).
- Guillery RW, Herrup K (1997) Quantification without pontification: Choosing a method for counting objects in sectioned tissues. *J Comp Neurol* 386:2–7.
- West MJ, Gundersen HJ (1990) Unbiased stereological estimation of the number of neurons in the human hippocampus. *J Comp Neurol* 296:1–22.
- Pakkenberg B, Gundersen HJ (1988) Total number of neurons and glial cells in human brain nuclei estimated by the disector and the fractionator. *J Microsc (Paris)* 150:1–20.
- Jayatissa MN, Henningsen K, West MJ, Wiborg O (2009) Decreased cell proliferation in the dentate gyrus does not associate with development of anhedonic-like symptoms in rats. *Brain Res* 1290:133–141.
- Gould E, Cameron HA (1997) Early NMDA receptor blockade impairs defensive behavior and increases cell proliferation in the dentate gyrus of developing rats. *Behav Neurosci* 111:49–56.
- Dayer AG, Ford AA, Cleaver KM, Yassaee M, Cameron HA (2003) Short-term and long-term survival of new neurons in the rat dentate gyrus. *J Comp Neurol* 460:563–572.
- Lister JP, et al. (2005) Effect of prenatal protein malnutrition on numbers of neurons in the principal cell layers of the adult rat hippocampal formation. *Hippocampus* 15:393–403.
- Olariu A, Cleaver KM, Cameron HA (2007) Decreased neurogenesis in aged rats results from loss of granule cell precursors without lengthening of the cell cycle. *J Comp Neurol* 501:659–667.
- Harburg GC, et al. (2007) Knockout of the mu opioid receptor enhances the survival of adult-generated hippocampal granule cell neurons. *Neuroscience* 144:77–87.
- Raff M (2003) Adult stem cell plasticity: Fact or artifact? *Annu Rev Cell Dev Biol* 19: 1–22.
- Kronenberg G, et al. (2003) Subpopulations of proliferating cells of the adult hippocampus respond differently to physiologic neurogenic stimuli. *J Comp Neurol* 467:455–463.
- Donovan MH, Yamaguchi M, Eisch AJ (2008) Dynamic expression of TrkB receptor protein on proliferating and maturing cells in the adult mouse dentate gyrus. *Hippocampus* 18:435–439.

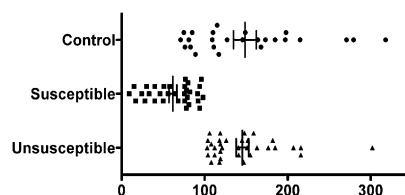


Fig. S1. Horizontal scatter plot depicting the distribution of interaction ratios 24 hr following social defeat stress for control, susceptible, and unsusceptible mice over multiple social defeat experiments [combined mice included in Fig. 1 C and E (+24 hr-P group)].

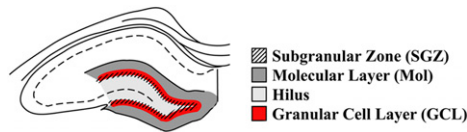


Fig. S2. Four regions of the dentate gyrus (–1.5 to –6.3 mm from bregma) were examined as previously described (1). These include the Mol, SGZ, oGCL (GCL is shaded red, whereas oGCL is the nonstriped red portion), and hilus. Details of regional assessment of cell counts are provided in main text and *SI Methods*.

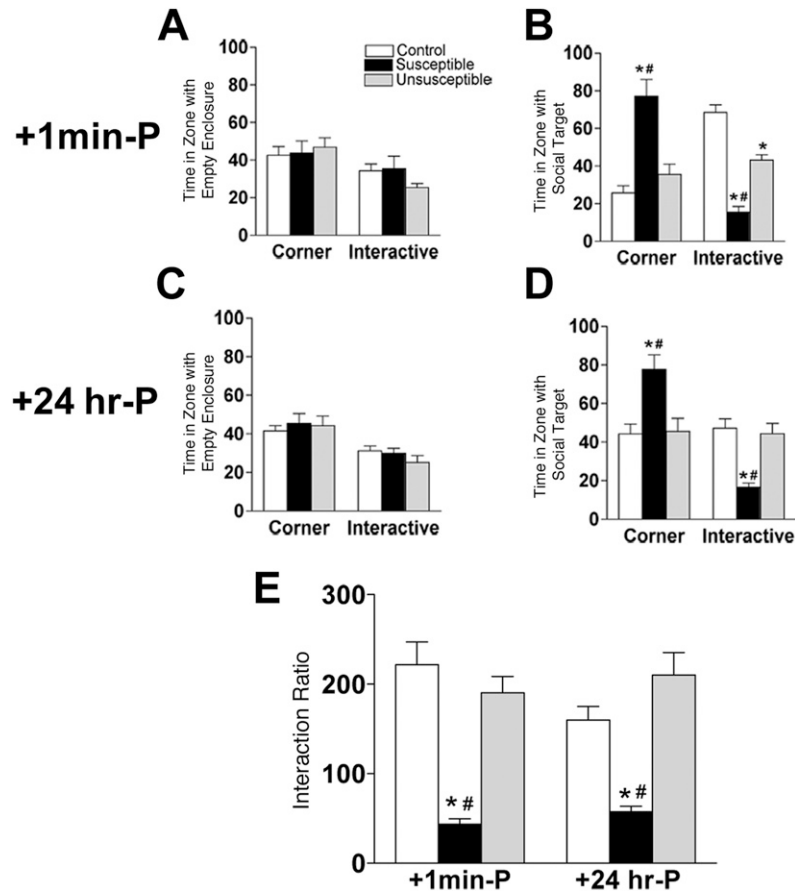


Fig. S3. Mice susceptible to defeat stress display similar social interaction 12 hr before (A and B; +1 min-P, $n = 9-18$ mice per group) or 12 hr after (B and C; +24 hr-P, $n = 7-12$ mice per group) day 10 of defeat. (A) Time (sec) spent in the corner ($F_{(2,37)} = 0.20$, $P = ns$) and within the interaction zone ($F_{(2,37)} = 2.42$, $P = ns$) in the +1 min-P group in the presence of an empty enclosure. (B) Time (sec) spent in the corners ($F_{(2,37)} = 16.5$, $P < 0.001$) and within the interaction zone ($F_{(2,37)} = 48.3$, $P < 0.001$) in the +1 min-P group in the presence of a social target. (C) Time (sec) spent in the corner ($F_{(2,64)} = 0.3$, $P = ns$) and within the interaction zone ($F_{(2,64)} = 1.0$, $P = ns$) in the +24 hr-P group in the presence of an empty enclosure. (D) Time (sec) spent in the corners ($F_{(2,64)} = 7.8$, $P < 0.005$) and within the interaction zone ($F_{(2,64)} = 12.1$, $P < 0.001$) in the +24 hr-P group in the presence of a social target. (E) Interaction ratio in both the +1 min-P and +24 hr-P experiments ($F_{(2,101)} = 35.1$, $P < 0.001$).

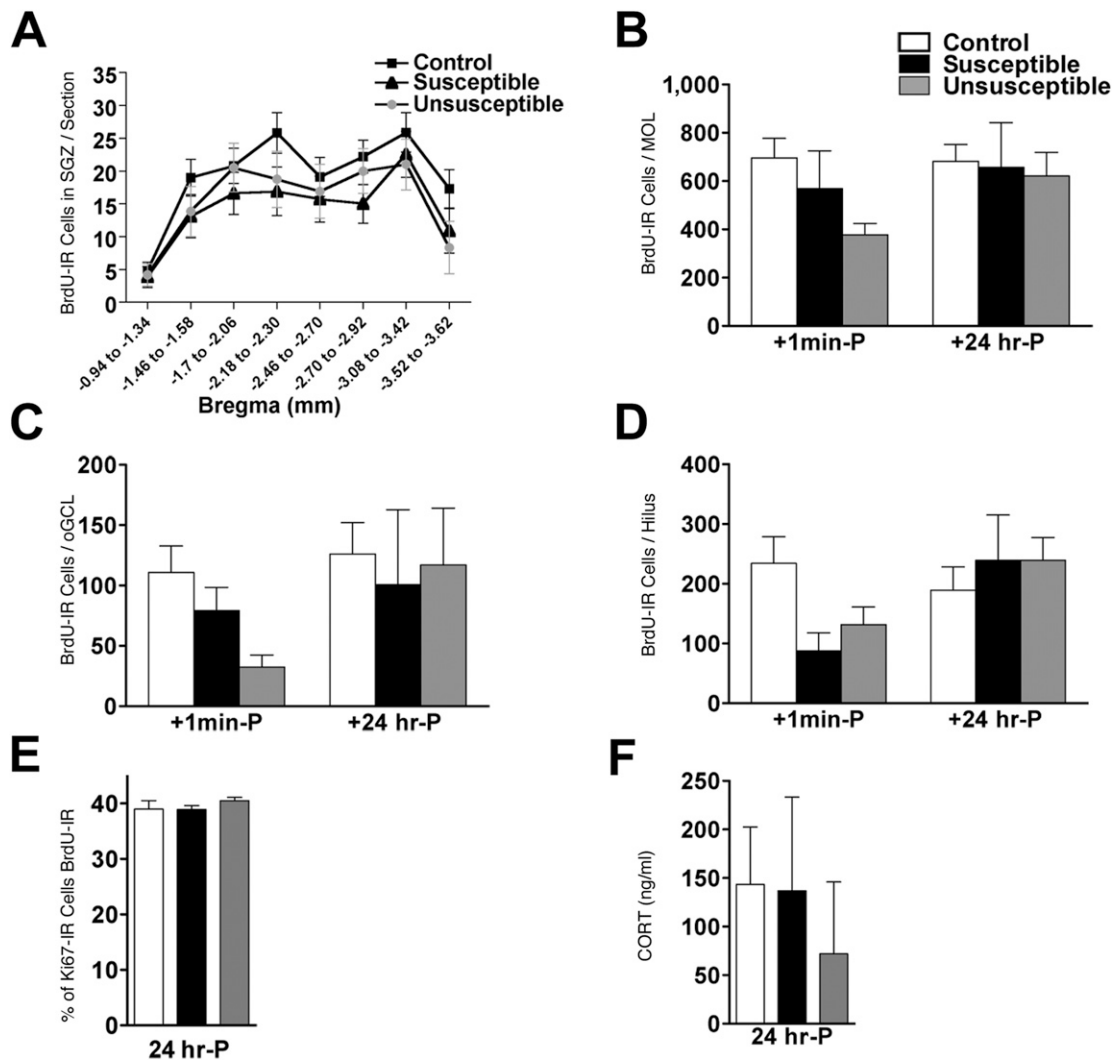


Fig. S4. Examination of BrdU-IR cells throughout the hippocampus immediately (+1 min-P) and 24 hr after (+24 hr-P) defeat stress. (A) BrdU-IR cell counts at different septotemporal locations throughout the dentate gyrus ($F_{(2,22)} = 2.2$, $P = ns$; $n = 6-11$ mice per group). (B) BrdU-IR cell counts in Mol ($F_{(2,50)} = 1.5$, $P = ns$). (C) BrdU-IR cell counts in oGCL ($F_{(2,50)} = 1.1$, $P = ns$). (D) BrdU-IR cell counts in hilus ($F_{(2,50)} = 0.6$, $P = ns$). (E) Percentage of Ki67-IR cells that are BrdU-IR in +24 hr-P group ($F_{(2,20)} = 0.4$, $P = ns$; $n = 5-10$ mice per group). (F) Serum CORT levels in mice 24 hr after last defeat ($F_{(2,22)} = 0.25$, $P = ns$; $n = 6-10$ mice per group).

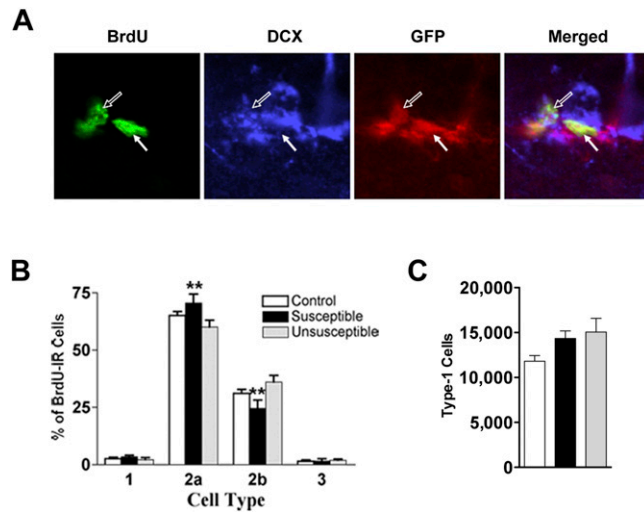


Fig. 58. Analysis of BrdU cells that are in distinct stages of neurogenesis (Type-1, Type-2a, Type-2b, and Type-3) in the nestin-GFP mice 24 hr after defeat stress (+24 hr-P). (A) Representative staining for BrdU-IR (green), DCX-IR (blue), and GFP-IR (red), with arrows highlighting Type-2a (GFP-IR/DCX⁻, closed arrow) and Type-2b cells (GFP-IR/DCX-IR, open arrow). (B) Susceptible mice had a significantly greater percentage of BrdU-IR cells that were Type-2a and a lower percentage of cells that were Type-2b compared with unsusceptible mice (main effect group: $F_{(2,80)} = 0.0$, $P = ns$; main effect phenotype: $F_{(3,80)} = 692.9$, $P < 0.0001$; group \times phenotype interaction: $F_{(6,80)} = 5.3$, $P < 0.01$; $n = 6$ – 10 mice per group). (C) Total number of Type-1 cells is not significantly different between the groups ($F_{(2,14)} = 3.4$, $P = ns$).

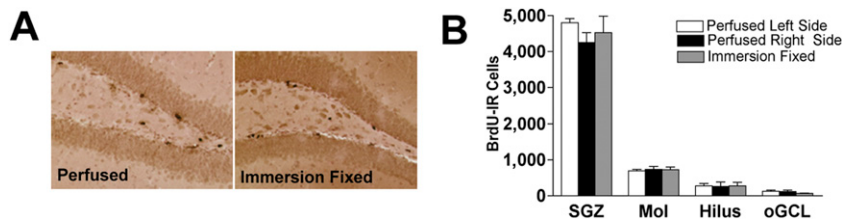


Fig. 59. Fixation (intracardial perfusion vs. immersion fixation) does not influence dentate gyrus BrdU-IR cell number. (A) Representative microphotograph of BrdU-IR cells in perfused vs. fixed tissue. (B) Number of BrdU-IR cells in the left or right side of a perfused brain when compared with an immersion fixed brain (main effect group: $F_{(2,21)} = 1.1$, $P = ns$; main effect region: $F_{(3,21)} = 302.1$, $P < 0.001$; group \times region: $F_{(6,21)} = 1.5$, $P = ns$; $n = 4$ mice per group). Regions are depicted in Fig. S2. Mean \pm SEM.